*Ecological Applications*, 22(1), 2012, pp. 166–183


# Demographic projection of high-elevation white pines infected with white pine blister rust: a nonlinear disease model

S. G. Field,[1,5] A. W. Schoettle,[2] J. G. Klutsch,[2,3] S. J. Tavener,[4] and M. F. Antolin[1]

[1]*Department of Biology, Colorado State University, Fort Collins, Colorado 80523-1878 USA*
[2]*Rocky Mountain Research Station, USDA Forest Service, Fort Collins, Colorado 80526 USA*
[3]*Department of Agricultural and Resource Economics, Colorado State University, Fort Collins, Colorado 80523 USA*
[4]*Department of Mathematics, Colorado State University, Fort Collins, Colorado 80523 USA*

*Abstract*. Matrix population models have long been used to examine and predict the fate of threatened populations. However, the majority of these efforts concentrate on long-term equilibrium dynamics of linear systems and their underlying assumptions and, therefore, omit the analysis of transience. Since management decisions are typically concerned with the short term (<100 years), asymptotic analyses could lead to inaccurate conclusions or, worse yet, critical parameters or processes of ecological concern may go undetected altogether.

We present a stage-structured, deterministic, nonlinear, disease model which is parameterized for the population dynamics of high-elevation white pines in the face of infection with white pine blister rust (WPBR). We evaluate the model using newly developed software to calculate sensitivity and elasticity for nonlinear population models at any projected time step. We concentrate on two points in time, during transience and at equilibrium, and under two scenarios: a regenerating pine stand following environmental disturbance and a stand perturbed by the introduction of WPBR.

The model includes strong density-dependent effects on population dynamics, particularly on seedling recruitment, and results in a structure favoring large trees. However, the introduction of WPBR and its associated disease-induced mortality alters stand structure in favor of smaller stages. Populations with infection probability ($\beta$) $\gtrsim 0.1$ do not reach a stable coexisting equilibrium and deterministically approach extinction.

The model enables field observations of low infection prevalence among pine seedlings to be reinterpreted as resulting from disease-induced mortality and short residence time in the seedling stage.

Sensitivities and elasticities, combined with model output, suggest that future efforts should focus on improving estimates of within-stand competition, infection probability, and infection cost to survivorship. Mitigating these effects where intervention is possible is expected to produce the greatest effect on population dynamics over a typical management timeframe.

*Key words:* Cronartium ribicola; *disease prevalence; elasticity; five-needle pine; nonlinear disease model;* Pinus albicaulis; Pinus flexilis; *sensitivity; stage-structured model.*

## Introduction

Infectious diseases, particularly introduced nonnative species, play an important role in the stability and ultimate fate of host species populations (Anderson and May 1986, Crowl et al. 2008). Mathematical models that include infection status and pathogen transmission aim to predict the trajectory of populations over time, highlight the most important parameters influencing dynamics of populations in the face of emerging pathogens, and constitute an important preliminary step for eventual management and/or policy decisions (e.g., Keane et al. 1996, Keeling et al. 2003). Models of infectious disease are often in the form of the three-class SIR (susceptible–infected–recovered) series of continuous-time differential equations (e.g., Anderson and May 1979; see Keeling and Rohani 2008), but discrete time models in the form of iterated maps (Oli et al. 2006) are also well suited to examine disease systems. More complex stage- or age-structured matrix models allow for inclusion of additional heterogenieties, such as differences in survival among reproductive and non-reproductive classes (Caswell 2001), and stage-specific nonlinearities like density dependence (Caswell 2008).

Efficient analysis of nonlinear multistage disease models can be achieved by calculating transient sensitivities and elasticities by use of the chain rule (Tavener et al., *in press*). Sensitivities, as well as sensitivity rescaled to reflect *relative* change (i.e., elasticities), provide insight into which model parameters must be estimated most accurately and which parameters can be approximated without losing model accuracy. Methods to analyze nonlinear matrix models (and generally, iterated maps) have been extended to allow the

Manuscript received 11 March 2011; revised 27 July 2011; accepted 18 August 2011. Corresponding Editor: A. D. McGuire.
[5] E-mail: sgf@colostate.edu

evaluation of sensitivity with respect to any parameter and at all time steps during population transience (Caswell 2008; Tavener et al., *in press*). Sensitivity during transience, defined as the trajectory (1) from arbitrary initial conditions toward a stable equilibrium solution, (2) following a disturbance, or (3) following a perturbation that changes the equilibrium solution, is of increasing interest to ecologists (Fox and Gurevitch 2000, Caswell 2007, Haridas and Tuljapurkar 2007). Transient analysis is especially important in applying models to management of infectious diseases because the time scale of management/conservation projects usually coincides with the short-term transient phase, rather than an equilibrium eventually reached in the long term (Ezard et al. 2010). Management activities are by definition short-term perturbations that require analysis of transient behavior, particularly in long-lived species.

Here we develop and apply a stage-structured population model to examine the effects of an introduced disease on the dynamics and stand structure of long-lived high-elevation, five-needle white pines (*Pinus albicaulis* and *P. flexilis*) in western North America. These species grow at or near the alpine treeline and play an important role in high-elevation ecosystems. They provide seed for a variety of subalpine wildlife species such as the Clark's Nutcracker, *Nucifraga columbiana* (Tomback 1982), squirrels and other rodents, and grizzly bears (Pease and Mattson 1999). These critical tree species, like all five-needle pines, are highly susceptible to white pine blister rust (Hoff and et al. 1980). In North America, white pine blister rust (WPBR) is caused by the nonnative fungal pathogen *Cronartium ribicola* and is lethal to high-elevation white pines as infected trees typically do not recover. Since its introduction to the western coast of British Columbia in ~1910 (Hoff and Hagle 1990), WPBR has gradually expanded southeast, inland and into the high-elevation Rocky Mountain ranges.

The emergence of the ecosystem management perspective in the 1990s shifted from managing forests for relatively few tree species that provide wood commodities to broader management of forests for ecosystem services. As a result, the importance of traditionally unmanaged high elevation white pine forests increased when it was recognized that they provide watershed protection and wildlife habitat (Schoettle 2004, Tomback and Achuff 2010). Management of WPBR in the high-elevation white pines now concentrates on both multigenerational population sustainability and understanding the effects of WPBR on short- and long-term population dynamics (Schoettle and Sniezko 2007). Previous modeling efforts in this pathosystem include both linear matrix models (Ettl and Cottone 2004) and nonlinear process models of fire succession that incorporate disease (Keane et al. 1996).

Considering the importance of transient sensitivity analysis to management decisions, we construct a nonlinear, stage-structured, SIR-type infection model and examine both transient and equilibrium sensitivity/elasticity. These results are useful in an applied conservation context to manage WPBR, identify critical parameters, and suggest future avenues of research.

## Methods

### *Model construction*

Because high-elevation white pines are long-lived species, predicting the effects of WPBR on forest dynamics depends on the development of disease models that incorporate nonlinear processes like density-dependent survival, seed dispersal, and seedling recruitment. We model a 1-ha, closed-system, high-elevation white pine population using a six-stage, nonlinear matrix projection model. Infection is included by allowing each stage to be either susceptible or infected with WPBR, resulting in a total of 12 stages. See Appendix A for details regarding parameter estimation and Appendix B for an explicit summary of modeling assumptions related to the system.

### *Generalized model framework*

We model a stage-structured population in the form of a nonlinear map. Vectors are indicated using the $\vec{v}$ notation, thus $\vec{x}$ is the state vector of the population and $x_i$, $i = 1, \ldots, N$, is the number of individuals in the $i$th stage. Matrices are indicated using capital bold fonts (e.g., **A**), and parameters of the model are represented by $\vec{p}_k$, $k = 1, \ldots, K$.

The elements of $\vec{x}_{\{n\}}(t) \in \mathbb{R}^n$ contain the population in each stage of a basic $n$-stage structured model at time $t$. The basic iterated map takes the following form:

$$\vec{x}_{\{n\}}(t+1, \vec{p}) = \vec{h}_{\{n\}}(\vec{x}_{\{n\}}(t, \vec{p}), \vec{p}) \tag{1}$$

$$\vec{x}_{\{n\}}(0, \vec{p}) = \vec{x}_{\{n\},0} \tag{2}$$

where $\vec{h}_{\{n\}}$: $\mathbb{R}^n \mapsto \mathbb{R}^n$. In *Incorporating disease*, we construct a general disease model from Eq. 1. We then separate the vector-valued function $\vec{h}_{\{n\}}$ into fecundity and survivorship and transition. For ease of exposition, we drop explicit dependence on $\vec{p}$ and let

$$\vec{x}_{\{n\}}(t+1) = \vec{g}_{\{n\}}(\vec{x}_{\{n\}}(t)) + \vec{f}_{\{n\}}(\vec{g}_{\{n\}}(\vec{x}_{\{n\}}(t))) \tag{3}$$

where $\vec{f}_{\{n\}}$ and $\vec{g}_{\{n\}}$ are vector-valued functions ($\mathbb{R}^n \mapsto \mathbb{R}^n$) that control fecundity and survivorship and transition, respectively.

*Incorporating disease.*—A typical SIR model with $n$ base individual stages has a total of $3n$ classes. Our model is atypical in that infection is neither density dependent (SI), nor frequency dependent (SI/$N$). This is because the life cycle of WPBR does not involve direct tree-to-tree infection, but rather the infection process occurs through an alternate host. Further, high-elevation white pines do not recover from infection and thus the model includes only susceptible and infected classes (i.e., no recovered class). Thus, we assume a constant background of infective spores and that the probability

TABLE 1. Survivorship ($s_i$) and transition ($t_i$) probabilities used in Eq. 17 and calculated using Eqs. 20 and 21.

| Stage | Class | Age | $s_i$ | $t_i$ |
|---|---|---|---|---|
| SEEDS | 1 | 0–1 | 0 | NL |
| $SD_1$ | 2 | 1–4 | 0.6360 (0.5888–0.6742) | 0.2120 (0.1962–0.2248) |
| $SD_2$ | 3 | 5–20 | 0.8391 (0.7238–0.9056) | 0.0559 (0.0482–0.0604) |
| SA | 4 | 21–40 | 0.9310 | 0.0490 |
| YA | 5 | 41–90 | 0.9653 (0.9575–0.9712) | 0.0197 (0.0195–0.0198) |
| MA | 6 | >90 | 0.9950 (0.9840–1.000) | |

*Notes:* See Table 2 for estimates of residence time ($R_i$) and mortality ($m_i$). We assume no seed bank; thus $s_1 = 0$ and $t_1$ in Eq. 17 is calculated via the nonlinear (NL) function in Eq. 29. Note that $s_6 = 1 - m_6$. Values in parentheses are 95% CI.

of infection is independent of the number of susceptible and infected individuals. The state vector becomes

$$\vec{x}_{\{2n\}} = \begin{pmatrix} \vec{x}^S_{\{n\}} \\ \vec{x}^I_{\{n\}} \end{pmatrix}. \tag{4}$$

We assume that the infection status affects survivorship and fecundity independently and let the cost of infection to survivorship and transition be $\mathbf{C}^{\nu}_{\{n\}}$, where

$$\mathbf{C}^{\nu}_{\{2n\}} = \begin{pmatrix} \mathbf{I}_{\{n\}} & \mathbf{0} \\ \mathbf{0} & \mathbf{C}^{\nu}_{\{n\}} \end{pmatrix} \qquad \mathbf{C}^{\nu}_{n} = \operatorname{diag}(c_i) \qquad i = 1, \ldots, n \tag{5}$$

where $\mathbf{I}_{(n)}$ is the $n \times n$ identity matrix. We define an intermediate, post-survival, population that has not yet undergone reproduction or infection as

$$\vec{y}_{\{2n\}} = \mathbf{C}^{\nu}_{\{2n\}} \times \vec{g}_{\{2n\}}(\vec{x}_{\{2n\}}). \tag{6}$$

The effect of infection on fecundity is modeled as a weighting of the infected individuals (i.e., infection cost). We define the nonlinear fecundity function

$$\vec{f}_{\{2n\}}: \mathbb{R}^{2n} \mapsto \mathbb{R}^{2n} \tag{7}$$

which we apply to the vector $\mathbf{C}^{\varphi}_{\{2n\}} \times \vec{y}_{\{2n\}}$, where $\mathbf{C}^{\varphi}_{\{2n\}}$ measures the cost of infection on the fecundity of infected individuals and

$$\mathbf{C}^{\varphi}_{\{2n\}} = \begin{pmatrix} \mathbf{I} & \mathbf{0} \\ \mathbf{0} & \mathbf{C}^{\varphi}_{\{n\}} \end{pmatrix}. \tag{8}$$

Lastly, infection is modeled by the linear operation

$$\mathbf{B}_{\{2n\}} \times \vec{x}_{\{2n\}} \tag{9}$$

where

$$\mathbf{B}_{\{2n\}} = \begin{pmatrix} \mathbf{I}_{\{n\}} - \mathbf{B}_{\{n\}} & \mathbf{0} \\ \mathbf{B}_{\{n\}} & \mathbf{I}_{\{n\}} \end{pmatrix} \qquad \mathbf{B}_{\{n\}} = \operatorname{diag}(\beta_i) \qquad i = 1, \ldots, n. \tag{10}$$

Once again $\mathbf{I}_{\{n\}}$ is the $n \times n$ identity matrix. Finally, combining Eqs. 6, 7, and 9 the complete general nonlinear map is given by

$$\vec{x}_{\{2n\}}(t+1) = \mathbf{B}_{\{2n\}} \times [(\vec{y}_{\{2n\}} + \vec{f}_{\{2n\}}(\mathbf{C}^{\varphi}_{\{2n\}} \times \vec{y}_{\{2n\}})]. \tag{11}$$

For the generalized case above, all three operations—the cost of infection to survival and transition, the cost of infection to fecundity, and infection probability—could be modeled as nonlinear processes.

### *The six-stage population model*

The pine population was subdivided into six stages: seeds, primary seedlings, secondary seedlings, saplings, young adults, and mature adults. We initially define the seed stage as 0–1 years. Other stages were identified from age and size dependent factors related to survival, reproductive capability and infection cost (Tomback et al. 1993, Smith and Hoffman 2000, 2001, Conklin 2004, Kegley and Sniezko 2004, Burns 2006, Smith et al. 2008), where age and size relationships were estimated from tree ring analysis (J. Coop and A. Schoettle, *unpublished data*). Primary seedlings ($SD_1$) are defined as 1–4 year olds, a period of low survivorship for most forest trees (Woodward 1987, Shepperd et al. 2006). By age 5, seedling survivorship increases (Maher and Germino 2006), and we define secondary seedlings ($SD_2$) as seedlings 5 years old until they reach a height of definable diameter at breast height (dbh; at 1.37 m). Based on age–height relationships for *P. flexilis* and *P. aristata* (J. Coop and A. Schoettle, *unpublished data*) this corresponds to ~20 years old. We define saplings (SA) as trees of 21 years (i.e., >1.37 m) until reproductive age, which we set at 40 years, since high-elevation white pines have first reproductive output between ages 30–50 (McCaughey and Schmidt 1990). We accordingly define young adults (YA) as reproductive trees ages 41–90 years and mature adults (MA) as greater than 90 years old with full reproductive capacity (Table 1). Delineation of YA and MA was estimated from field observations of reproductive capacity, and age/size measurements from *P. flexilis* (Burns et al. 2011; J. Coop and A. Schoettle, *unpublished data*). Based on this stage structure, the mean dbh for saplings, young adults, and mature adults was estimated to be 2.05, 12.5, and 37.0 cm respectively (Table 2).

For each iteration of the map we assume the following sequence of biological events (changing this order implicitly changes model assumptions and thus alters the model): calculation of LAI ($\vec{x}$) (Eq. 25), seedling recruitment (Eq. 30), survival and transition (Eq. 17),

TABLE 2. Parameters used in the model.

| Parameter | $p_k$ | Symbol | Default value | 95% CI |
|---|---|---|---|---|
| Mortality SEEDS | | $m_1$ | 1 | |
| Mortality $SD_1$ | 1 | $m_2$ | 0.152 | 0.101–0.215 |
| Mortality $SD_2$ | 2 | $m_3$ | 0.105 | 0.034–0.228 |
| Mortality SA | 3 | $m_4$ | 0.020 | |
| Mortality YA | 4 | $m_5$ | 0.015 | 0.009–0.023 |
| Mortality MA | 5 | $m_6$ | 0.005 | 0.000–0.016 |
| Residence time SEEDS | | $R_1$ | 1 | |
| Residence time $SD_1$ | 6 | $R_2$ | 4 | |
| Residence time $SD_2$ | 7 | $R_3$ | 16 | |
| Residence time SA | 8 | $R_4$ | 20 | |
| Residence time YA | 9 | $R_5$ | 50 | |
| Residence time MA | | $R_6$ | $\infty$ | |
| Transmission probability | 10–14 | $\beta_2, \ldots, \beta_6$ | 0.044 | 0.037–0.052 |
| Mean dbh SA | 15 | $d_4$ | 2.05 | |
| Mean dbh YA | 16 | $d_5$ | 12.5 | |
| Mean dbh MA | 17 | $d_6$ | 37.0 | |
| Infection cost ($SD_1$) | 18 | $c_2$ | 0.01 | 0–0.03 |
| Infection cost ($SD_2$) | 19 | $c_3$ | 0.13 | 0.10–0.16 |
| Infection cost (viability) | 20 | $\delta$ | 0.15 | |
| LA $SD_2$ | 21 | $\alpha_1$ | 0.456 | |
| LA coefficient 1 | 22 | $\alpha_2$ | 0.0736 | 0.011–2.701 |
| LA coefficient 2 | 23 | $\alpha_3$ | 2.070 | 1.932–5.220 |
| Background LAI | 24 | $\mathrm{LAI_b}$ | 0 | |
| Maximum cones per tree | 25 | $C_{\max}$ | 7.5 | |
| No. seeds per cone | 26 | $S_{\text{cone}}$ | 46 | |
| Infection cost (fecundity) | 27 | $C_f$ | 0.125 | |
| No. Clark's Nutcrackers | 28 | nBirds | 3 | |
| Proportion of seeds found | 29 | $P_{\text{find}}$ | 0.8 | |
| Proportion of seeds consumed | 30 | $P_{\text{cons}}$ | 0.3 | |
| No. seeds per cache | 31 | SpC | 3.7 | |
| Fecundity ratio (YA : MA) | | $\rho$ | 0.1 | |

*Notes:* The parameter numbers ($p_k$, $k = 1, \ldots, 31$) correspond to the sensitivity and elasticity analysis. The 95% CIs are from the maximum-likelihood estimates (MLE). Abbreviations are: $SD_1$, primary seedlings; $SD_2$, secondary seedlings; SP, saplings; YA, young adults; MA, mature adults; LA, leaf area; dbh, diameter at breast height.

calculation of LAI ($\vec{y}$) (Eq. 25), fecundity (Eq. 33), and finally infection (Eq. 43).

*Mathematical description.*—Let $x_i$ denote the number of individuals in stage $i$ where $i = 1, \ldots, 6$. Let the elements of $\vec{x}_{\{6\}}(t) \in \mathbb{R}^6$ contain the populations in each stage of a six-stage structured model at time $t$:

$$\vec{x}_{\{6\}} = \begin{pmatrix} \text{SEEDS} \\ \text{SD}_1 \\ \text{SD}_2 \\ \text{SA} \\ \text{YA} \\ \text{MA} \end{pmatrix} = \begin{pmatrix} x_1 \\ x_2 \\ x_3 \\ x_4 \\ x_5 \\ x_6 \end{pmatrix}. \tag{12}$$

We define the following nonlinear map:

$$\vec{x}_{\{6\}}(t+1) = \vec{g}_{\{6\}}[\vec{x}_{\{6\}}(t)] + \vec{f}_{\{6\}}\left(\vec{g}_{\{6\}}[\vec{x}_{\{6\}}(t)]\right) \tag{13}$$

where $\vec{f}$ and $\vec{g}$ represent vector-valued functions that control fecundity and survivorship and transition functions, respectively.

*Linear model components: survivorship and transition.*—We model fecundity and seedling recruitment as nonlinear processes, while survivorships and transitions are assumed to be linear. Correspondingly, we split $\vec{g}_{\{6\}}(\vec{x}_{\{6\}})$ into linear and nonlinear components. We discuss nonlinear components in *Nonlinear model components: density-dependence*. Let

$$\vec{g}_{\{6\}}(\vec{x}_{\{6\}}) = \mathbf{S}_{\{6\}} \times \left(\vec{x}_{\{6\}} + \vec{\gamma}_{\{6\}}(\vec{x}_{\{6\}})\right) \tag{14}$$

where $\mathbf{S}_{\{6\}}$ is the linear survivorship matrix (defined in Eq. 17), and $\vec{\gamma}_{\{6\}}(\vec{x}_{\{6\}})$ represents a vector-valued nonlinear function acting upon $\vec{x}_{\{6\}}$, which defines the transition from SEED to $SD_1$ recruitment process described in *Nonlinear model components: density-dependence* and defined in Eq. 30. For notational convenience, we let

$$\vec{\hat{x}}_{\{6\}} = \vec{x}_{\{6\}} + \vec{\gamma}_{\{6\}}(\vec{x}_{\{6\}}) \tag{15}$$

to define

$$\vec{g}_{\{6\}}(\vec{x}_{\{6\}}) = \mathbf{S}_{\{6\}} \times \vec{\hat{x}}_{\{6\}} = \vec{y}_{\{6\}} \tag{16}$$

where $\vec{y}_{\{6\}}$ represents an intermediate population. The projection matrix $\mathbf{S}_{\{6\}}$ is

$$\mathbf{S}_{\{6\}} = \begin{pmatrix} 0 & 0 & 0 & 0 & 0 & 0 \\ 0 & s_2 & 0 & 0 & 0 & 0 \\ 0 & t_2 & s_3 & 0 & 0 & 0 \\ 0 & 0 & t_3 & s_4 & 0 & 0 \\ 0 & 0 & 0 & t_4 & s_5 & 0 \\ 0 & 0 & 0 & 0 & t_5 & s_6 \end{pmatrix} \tag{17}$$

with the following coefficients along the diagonal:

$$s_1 = 0 \qquad s_2 = 0.636 \qquad s_3 = 0.8391$$
$$s_4 = 0.9310 \qquad s_5 = 0.9653 \qquad s_6 = 0.995 \qquad (18)$$

and, along the sub-diagonal,

$$t_1 = 0 \qquad t_2 = 0.212 \qquad t_3 = 0.0559$$
$$t_4 = 0.0490 \qquad t_5 = 0.0197. \qquad (19)$$

The $S_{21}$ ($t_1$) and $S_{11}$ ($s_1$) entries are both 0 since the germination and production of seeds are modeled as nonlinear processes and are included later when nonlinearities are calculated in *Nonlinear model components*. We assume seeds either germinate to primary seedlings or become nonviable within one year (i.e., no seed bank). Thus, $s_1 = 0$; see Eq. 17.

Survivorship and transition (i.e., viability) probabilities for primary seedlings through mature adults were calculated as

$$s_i = \left(1 - \frac{1}{R_i}\right) \times (1 - m_i) \qquad i = 2, \ldots, 6 \qquad (20)$$

$$t_i = \frac{1}{R_i} \times (1 - m_i) \qquad i = 2, \ldots, 5 \qquad (21)$$

where $s_i$ is the proportion of individuals surviving and remaining in the same stage $i$, $t_i$ is the proportion of individuals within stage $i$ that grow into the next stage, $R_i$ is the residence time for stage $i$, and $m_i$ is the mortality of stage $i$ individuals. Note that the entries $t_i$ reflect the combination of transition and survivorship from stage $i \rightarrow i + 1$, such that survivorship is contained *within* the transition probability. Table 1 shows the calculated values for $s_i$ and $t_i$. See Table 2 for $m_i$ and $R_i$ values.

*Nonlinear model components: density-dependence.*—Modeling density dependence is inherently nonlinear because the previous population ($\vec{x}(t, \vec{p})$) vector affects current parameters, and because the population depends implicitly upon time. There are two forms of density dependence: seedling recruitment (i.e., germination) and fecundity (i.e., female production of seed/cones).

Leaf area index (LAI), the amount of projected leaf area over a given ground area, is commonly used to reflect vegetation density (Steltzer and Welker 2006) and relates to ecosystem parameters like carbon, water and energy flux, and competitive interactions between and within species. Here, density-dependent processes are mediated via LAI. Lower values of LAI represent sparsely populated stands whereas larger LAI values represent more dense, shaded ones. Typical LAI estimates, depending on succession stage, environmental conditions, and species of interest, plateau at approximately 9 for numerous ecosystems (Gower et al. 1999). Pine forests, however, rarely exceed an LAI of 8 (Brown 2001) and Law et al. (2001) estimated the range for *P. ponderosa* as 0.59–2.77. Our equilibrium values of LAI without and with infection were 4.71 and 2.49, respectively, which is in accordance with these estimates. Perhaps most importantly, at no point during the path to equilibrium does LAI exceed 5.0, well within the reported upper threshold for pine ecosystems.

The relationship between leaf area (LA) and diameter at 1.37 m (dbh) was estimated by maximum-likelihood estimation (MLE) assuming the general form $y = ax^b$ fit to data from Callaway et al. (2000) and supplemented with data for *P. albicaulis* (A. Sala, *unpublished data*). Leaf area was calculated using Eqs. 23 and 24. MLE and 95% confidence intervals for $\alpha_2$ and $\alpha_3$ are shown in Table 2. Primary seedlings have negligible LA and thus do not contribute to LAI. For secondary seedlings, a LA estimate of 0.456 $m^2$ was estimated from data in Schoettle and Rochelle (2000) and Schoettle (1994) because this stage is below 1.37 m in height (and therefore dbh = 0).

To determine LAI at a given time step, LA by stage was calculated and multiplied by the number of individuals present in each stage, then summed to obtain the total LA of the population. This value was divided by land area (10 000 $m^2$) to obtain LAI. Finally, because natural populations are seldom monocultures, $LAI_b$ was added to represent background interspecific competition contributed by leaf cover of other tree species.

Specifically, the LA for each stage is calculated as a function of the diameter at breast height (1.37 m) according to Eq. 23. The contributions of each stage to the overall leaf area index are weighted by the populations within each stage and then scaled by the area in Eq. 25. Secondary seedlings have $d_3 = 0$ but we assume they contribute to stand leaf area, thus $l_3$ is defined as the constant $\alpha_1$. Using the mean dbh measurements for the six stages,

$$d_1 = 0 \qquad d_2 = 0 \qquad d_3 = 0$$
$$d_4 = 2.05 \qquad d_5 = 12.5 \qquad d_6 = 37.0 \qquad (22)$$

and

$$l_1 = 0 \qquad l_2 = 0 \qquad l_3 = \alpha_1$$
$$l_i = \alpha_2 (d_i)^{\alpha_3} \qquad i = 4, \ldots, 6 \qquad (23)$$

where

$$\alpha_1 = 0.456 \qquad \alpha_2 = 0.0736 \qquad \alpha_3 = 2.070. \qquad (24)$$

We calculate LAI as

$$\mathrm{LAI}(\vec{x}_6) = \frac{(\vec{l}, \vec{x}_{\{6\}})}{10\,000} + \mathrm{LAI_b} \qquad (25)$$

where $(\vec{a}, \vec{b})$ denotes the inner product $\vec{a}^\top \times \vec{b}$.

*Nonlinear model components: seedling recruitment.*—We model the transition of the SEED $\rightarrow$ $SD_1$ ($t_1$) as a density-dependent process. Seed germination depends upon a number of factors including seed production, predation, dispersal, environmental conditions, and seedbed conditions (Woodward 1987, Keane et al.

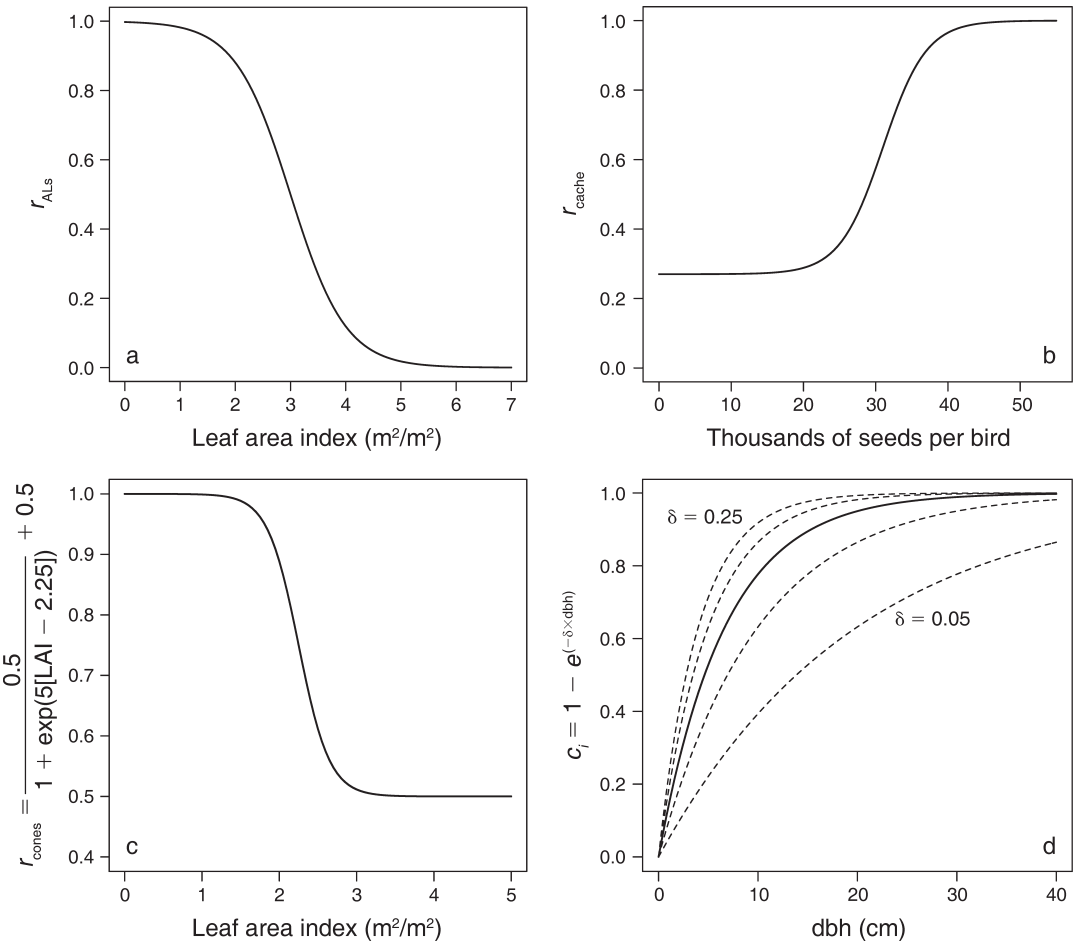


FIG. 1. Reduction factors for (a, b) seedling recruitment, (c) fecundity, and (d) infection cost. The cost of infection, $c_i$, is a function of tree size, $c_{4\rightarrow 6}$. Lines represent $\delta = 0.05$, 0.10, 0.15, 0.20, and 0.25, where $\delta$ is a coefficient used to determine the strength of the infection cost to survivorship. The default value is $\delta = 0.15$ (solid line). Higher $\delta$ values shift curves closer to 1.0 and thus exhibit a lower cost to survivorship. Reduction factors are: $r_{\text{ALs}}$, a reduction factor related to available light; $r_{\text{cache}}$, a reduction factor related to the "cacheability" of seeds by birds; and $r_{\text{cones}}$, a reduction factor related used modify the maximum number of cones a tree can produce in a given year.

1990, Ettl and Cottone 2004). We modified a germination equation from Keane et al. (1990) to obtain the germination probability in Eq. 29. First, we define

$$\text{SpB}(\vec{x}_{\{6\}}) = \frac{x_1}{\text{nBirds}} \tag{26}$$

$$r_{\text{cache}}(\vec{x}_{\{6\}}) = \frac{0.73}{1 + \exp\Big((31000 - \text{SpB}(\vec{x}_{\{6\}}))/3000\Big)} + 0.27 \tag{27}$$

$$r_{\text{ALs}}(\vec{x}_{\{6\}}) = \frac{1}{1 + \exp\Big(2(\text{LAI}(\vec{x}_{\{6\}}) - 3)\Big)} \tag{28}$$

where $x_1$ is the number of seeds at time $t$, nBirds is the number of Clark's Nutcrackers per hectare, SpB is the number of seeds per bird, $r_{\text{cache}}$ is a reduction factor for the propensity to cache seeds, and $r_{\text{ALs}}$ is a reduction factor for the available light and is directly dependent upon LAI. The functions for $r_{\text{ALs}}$ and $r_{\text{cache}}$ are plotted in Fig. 1a and 1b, respectively. See Appendices A and B for further description and derivation of these two density-dependent reduction factors.

Finally, the probability of seeds germinating in a given year is defined by

$$r_2(\vec{x}_{\{6\}}) = \left[\frac{(1 - P_{\text{find}})(1 - P_{\text{cons}})}{\text{SpC}}\right] \times r_{\text{cache}}(\vec{x}_{\{6\}}) \times r_{\text{ALs}}(\vec{x}_{\{6\}}). \tag{29}$$

The following parameters are independent of population size: $P_{\text{cons}}$, the proportion of seeds consumed by nutcrackers during a caching season (R. Keane, *personal communication*, in Cottone 2001; vander Wall 1988),

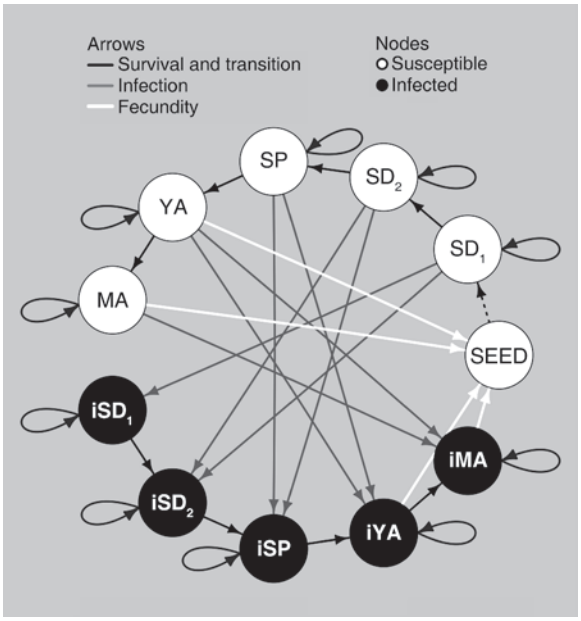


FIG. 2. Life-cycle graph of the high-elevation white pine disease model. The cycle begins with seed (SEED) and moves counter-clockwise to mature adults (MA). Other abbreviations are: $SD_1$, primary seedlings; $SD_2$, secondary seedlings; SP, saplings; and YA, young adults. The prefix "i" denotes infected individuals. White nodes represent susceptible stages; black nodes represent infected stages. Black arrows represent either survivorship or transitions, gray arrows represent infection processes, and white arrows represent the fecundity process. The transition arrow from SEED $\rightarrow$ $SD_1$ is dotted to emphasize the fact that germination is a density-dependent process and therefore differs from the other black arrows (which represent linear processes).

$P_{\text{find}}$, the proportion of seeds reclaimed from caches by the nutcrackers, and SpC, the average seeds per cache (range = 2.6–5.0; vander Wall and Balda 1977, Tomback 1982, vander Wall 1988, Tomback et al. 2005; see Table 2). The number of new seedlings is then given by

$$\vec{\gamma}_{\{6\}}(\vec{x}_{\{6\}}) = r_2(\vec{x}_{\{6\}}) \times x_1 \times \vec{e}_2 \tag{30}$$

where $\vec{e}_2 \in \mathbb{R}^6$ is the unit vector with a single nonzero entry in the second position.

*Nonlinear model components: fecundity*.—We assume that fecundity differences arise entirely through cone production and that pollen is non-limiting (see Appendix B; item 8). We assume only YA and MA stages (>40 yr) produce cones. The yearly maximum number of cones per MA individual was defined as $C_{\max} = 7.5$ (Schwartz et al. 2006) and is consistent with data from McKinney and Tomback (2007). We further assume YA individuals produce a maximum of 10% ($\rho = 0.1$) of a MA individual (J. Coop and A. Schoettle, *unpublished data*; calculated from primary data from Burns [2006]).

The number of cones is a function of the number of young and mature adults and their total fecundity. Seed production is determined by the number of seeds per cone, $S_{\text{cone}}$, and the number of cones per tree, $C_{\text{tree}}(\vec{y}_{\{6\}})$. We define

$$C_{\text{tree}}(\vec{y}_{\{6\}}) = \left[\frac{0.5}{1 + \exp(5(\text{LAI}(\vec{y}_{\{6\}}) - 2.25))} + 0.5\right] \times C_{\max}$$
$$= r_{\text{cones}} \times C_{\max} \tag{31}$$

$$r_1(\vec{y}_{\{6\}}) = S_{\text{cone}} \times C_{\text{tree}}(\vec{y}_{\{6\}}) \tag{32}$$

where $C_{\max}$ and $S_{\text{cone}}$ are fecundity parameters (Table 2). The function for $r_{\text{cones}}$ is plotted in Fig. 1c. The number of seeds produced is given by

$$\vec{f}_{\{6\}}(\vec{y}_{\{6\}}, \rho) = r_1(\vec{y}_{\{6\}}) \times (\rho \times y_5 + y_6) \times \vec{e}_1 \tag{33}$$

where $\vec{e}_1 \in \mathbb{R}^6$ is a unit vector with a single nonzero entry in the first position, $\rho$ is the reduction in seed production of YA relative to MA, and $\vec{y}_{\{6\}}$, the intermediate population vector, is defined in Eq. 16.

*The six-stage nonlinear map*.—Combining Eqs. 15, 16, 30, and 33 obtains the six-stage, nonlinear map of the population without infection dynamics

$$\vec{x}_6(t+1) = \vec{y}_{\{6\}} + \vec{f}_{\{6\}}(\vec{y}_{\{6\}}, \rho). \tag{34}$$

### *The 12-stage disease model*

When incorporating disease we assume all stages except seeds are susceptible to infection (i.e., $x_7 = 0$). See Fig. 2 for a description of the life cycle graph for the full 12-stage model. Including disease doubles the number of stages, as described in *Incorporating disease*, and we define

$$\vec{x}_{(12)} = \begin{pmatrix} \vec{x}^{\text{S}}_{\{6\}} \\ \vec{x}^{\text{I}}_{\{6\}} \end{pmatrix} = \begin{pmatrix} \text{SEEDS} \\ \text{susceptible } SD_1 \\ \text{susceptible } SD_2 \\ \text{susceptible SA} \\ \text{susceptible YA} \\ \text{susceptible MA} \\ 0 \\ \text{infected } SD_1 \\ \text{infected } SD_2 \\ \text{infected SA} \\ \text{infectedYA} \\ \text{infected MA} \end{pmatrix} = \begin{pmatrix} x_1 \\ x_2 \\ x_3 \\ x_4 \\ x_5 \\ x_6 \\ x_7 \\ x_8 \\ x_9 \\ x_{10} \\ x_{11} \\ x_{12} \end{pmatrix}. \tag{35}$$

*Survivorship, transition, and disease*.—We define

$$\vec{g}_{(12)}(\vec{x}_{\{12\}}) = \vec{g}_{\{12\}} \begin{pmatrix} \vec{x}^{\text{S}}_{\{6\}} \\ \vec{x}^{\text{I}}_{\{6\}} \end{pmatrix} \tag{36}$$

as follows. The nonlinear transition function for seedling recruitment $\vec{\gamma}_{\{6\}}$ is described in *Nonlinear model components: density-dependence*. Certain components of this function (e.g., LAI and SpB) are independent of disease status and must be extended to be functions of $\vec{x}_{\{12\}}$.

Similarly, the fecundity function $r_1(\cdot)$ as described in *Nonlinear model components: density-dependence* must be extended to be a function of $\vec{y}_{\{12\}}$. Let

$$\vec{\hat{x}}_{\{12\}} = \begin{pmatrix} \vec{x}^{\,S}_{\{6\}} \\ \vec{x}^{\,I}_{\{6\}} \end{pmatrix} + \begin{pmatrix} \vec{\gamma}^{\,SI}_{\{6\}}(\vec{x}^{\,S}_{\{6\}}, \vec{x}^{\,I}_{\{6\}}) \\ 0 \end{pmatrix} \tag{37}$$

where the nonlinear function $\vec{\gamma}^{\,SI}_{\{6\}}$ is the modification of $\vec{\gamma}_{\{6\}}$. Since there are no infected seeds, infected $SD_1$ individuals cannot arise via seedling recruitment. We define

$$\begin{aligned} \vec{g}_{\{12\}} &= \begin{pmatrix} \mathbf{S}_{\{6\}} & \mathbf{0} \\ \mathbf{0} & \mathbf{S}_{\{6\}} \end{pmatrix} \times \begin{pmatrix} \mathbf{I}_{\{6\}} & \mathbf{0} \\ \mathbf{0} & \mathbf{C}^{v}_{\{6\}} \end{pmatrix} \times \begin{pmatrix} \vec{\hat{x}}^{\,S}_{\{6\}} \\ \vec{\hat{x}}^{\,I}_{\{6\}} \end{pmatrix} \\ &= \mathbf{S}_{\{12\}} \times \mathbf{C}^{v}_{\{12\}} \times \vec{\hat{x}}_{\{12\}} = \vec{y}_{\{12\}}. \end{aligned} \tag{38}$$

The viability cost of infection is

$$\mathbf{C}^{v}_{\{12\}} = \begin{pmatrix} \mathbf{I}_{\{6\}} & \mathbf{0} \\ \mathbf{0} & \mathbf{C}^{v}_{\{6\}} \end{pmatrix} \tag{39}$$

where

$$\mathbf{C}^{v}_{\{6\}} = \begin{pmatrix} 0 & 0 & 0 & 0 & 0 & 0 \\ 0 & c_2 & 0 & 0 & 0 & 0 \\ 0 & 0 & c_3 & 0 & 0 & 0 \\ 0 & 0 & 0 & c_4 & 0 & 0 \\ 0 & 0 & 0 & 0 & c_5 & 0 \\ 0 & 0 & 0 & 0 & 0 & c_6 \end{pmatrix}$$

and the cost of infection is either a constant (for stages without a definable dbh) or a function of dbh (SA, YA, and MA). Specifically, the viability cost reduction coefficients are

$$c_1 = 0 \qquad c_2 = 0.01 \qquad c_3 = 0.13 \tag{40}$$

$$c_i = 1 - \exp(-\delta \times d_i) \qquad i = 4, \ldots, 6 \tag{41}$$

and the parameter $\delta$ is a coefficient that influences the cost of infection for trees taller than 1.37 m. The matrix product $\mathbf{S}_{\{12\}} \times \mathbf{C}^{v}_{\{12\}}$ in Eq. 38 is post-multiplied because we assume transition from stage $i \rightarrow i+1$ occurs *after* survivorship (see Appendix B for additional details).

*Fecundity and disease.*—White pine blister rust is not vertically transmitted from adults to seeds, therefore both susceptible and infected adults produce susceptible seeds. Infection with WPBR reduces cone production only since there is no evidence for reduced pollen production with WPBR infection. We again assume pollen is non-limiting and that fecundity of infected YA and MA are reduced by the same proportion ($C_f$; Table 2). Fecundity for the 12-stage model is defined by

$$\begin{aligned} &\vec{f}_{\{12\}}(\vec{y}_{\{12\}}, \rho, C_f) \\ &\quad = r_1(\vec{y}_{\{12\}}) \times ((\rho y_5 + y_6) + C_f(\rho y_{11} + y_{12})) \times \vec{e}_1 \end{aligned} \tag{42}$$

where, as with the six-stage model, $\rho$ is a measure of the effect of stage-class on fecundity and $C_f$ is the effect of infection on fecundity (compare Eq. 33). Now $\vec{e}_1 \in \mathbb{R}^{12}$ is a unit vector with a single nonzero entry in the first position.

*Infection.*—Simplifying assumptions about WPBR infection of high-elevation white pines were implemented. We model disease prevalence assuming the probability of infection is constant and is independent of stage, time, and the solution. We define

$$\mathbf{B}_{\{12\}} = \begin{pmatrix} \mathbf{I}_{\{6\}} - \mathbf{B}_{\{6\}} & \mathbf{0} \\ \mathbf{B}_{\{6\}} & \mathbf{I}_{\{6\}} \end{pmatrix} \tag{43}$$

where

$$\mathbf{B}_{\{6\}} = \begin{pmatrix} 0 & 0 & 0 & 0 & 0 & 0 \\ 0 & \beta_2 & 0 & 0 & 0 & 0 \\ 0 & 0 & \beta_3 & 0 & 0 & 0 \\ 0 & 0 & 0 & \beta_4 & 0 & 0 \\ 0 & 0 & 0 & 0 & \beta_5 & 0 \\ 0 & 0 & 0 & 0 & 0 & \beta_6 \end{pmatrix}$$

where the infection probability is

$$\beta_1 = 0 \qquad \beta_2 = \beta_3 = \beta_4 = \beta_5 = \beta_6 = 0.044. \tag{44}$$

Note that both $c_1 = 0$ and $\beta_1 = 0$ to emphasize that seeds cannot become infected.

*The 12-stage nonlinear map.*—The matrices $\mathbf{B}_{\{12\}}$, $\mathbf{C}^{v}_{\{12\}}$, and $\mathbf{S}_{\{12\}}$ are independent of both the solution and time. We also emphasize that the order of biological events reflect that infection occurs after seedling recruitment, survivorship and transition, and fecundity. Thus, infection is the final process and combining Eqs. 37, 38, 42, and 43, we obtain the 12-stage, nonlinear map

$$\vec{x}_{12}(t+1) = \mathbf{B}_{\{12\}} \times \left(\vec{y}_{\{12\}} + \vec{f}_{\{12\}}(\vec{y}_{\{12\}}, \rho, C_f)\right). \tag{45}$$

### *Sensitivity analysis*

Sensitivity and elasticity analyses were performed using the software package SENSAI (Tavener et al., *in press*), which analyzes deterministic, multistage, multiparameter, nonlinear, population models. This program efficiently calculates sensitivity at all time points during transience, rather than focusing on long-term asymptotic dynamics, which, as noted earlier, may result in misleading conclusions that affect management decisions (Fox and Gurevitch 2000, Ezard et al. 2010). The basic nonlinear iterative process is

$$\vec{x}(t+1, \vec{p}) = \vec{h}(\vec{x}(t, \vec{p}), \vec{p}) \qquad t > 0$$

$$\vec{x}(0) = \vec{z}. \tag{46}$$

Using index notation, we rewrite Eq. 46 as

$$x_i = h_i(\vec{x}, \vec{p}) \qquad i = 1, \ldots, N. \tag{47}$$

Differentiating Eq. 47 with respect to parameters, $p_k$, gives the following:

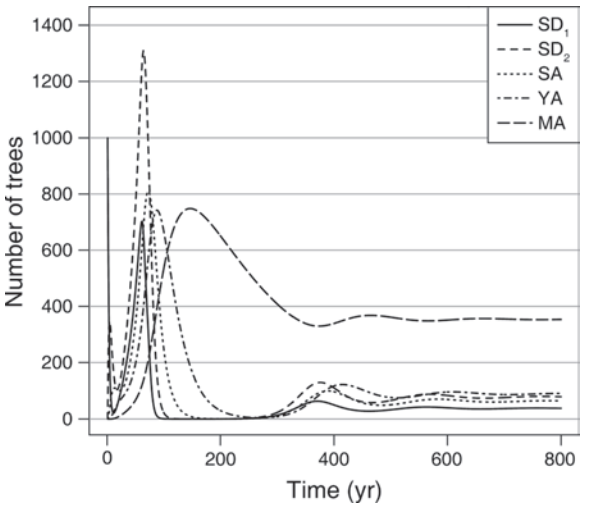


FIG. 3. Population projection of a pine stand to equilibrium with parameter defaults (see Table 2) and without disease (disease transmission probability $\beta_i = 0$; stage $i = 2, \ldots, 6$), regenerated from 1000 $SD_1$ individuals (seed population, $x_1$, is not shown).

$$\frac{\partial x_i(t+1)}{\partial p_k} = \sum_{m=1}^{N} \frac{\partial h_i}{\partial x_m} \times \frac{\partial x_m(t)}{\partial p_k} + \frac{\partial h_i}{\partial p_k}$$
$$\frac{\partial x_i(0)}{\partial p_k} = 0 \qquad (48)$$
$$i = 1, \ldots, N \quad k = 1, \ldots, K.$$

Observe that to evolve Eq. 48 to determine the stability of $x_i$ with respect to $p_k$ at any $t > 0$, we need to evaluate $\partial h_i/\partial x_m$ and $\partial h_i/\partial p_k$.

To determine stability with respect to the initial conditions, we differentiate Eq. 47 with respect to the initial conditions to give

$$\frac{\partial x_i(t+1)}{\partial z_k} = \sum_{m=1}^{N} \frac{\partial h_i}{\partial x_m} \times \frac{\partial x_m(t)}{\partial z_k} + \frac{\partial h_i}{\partial z_k}$$
$$\frac{\partial x_i(0)}{\partial z_i} = 1 \qquad (49)$$
$$\frac{\partial x_i(0)}{\partial z_k} = 0 \quad k \neq i$$
$$i = 1, \ldots, N \quad k = 1, \ldots, N.$$

or alternatively using the *Kronecker delta*,

$$\frac{\partial x_i(0)}{\partial z_j} = \delta_{ij}$$

where

$$\delta_{ij} = \begin{cases} 1 & \text{if } i = j \\ 0 & \text{otherwise.} \end{cases} \qquad (50)$$

To solve for the population and its stability with respect to parameters and initial conditions we evolve Eqs. 47, 48, and 49 simultaneously.

Elasticities are defined in terms of relative sensitivities. Let

$$\Delta\xi = \frac{\Delta x}{x} \qquad \Delta\kappa = \frac{\Delta p}{p}.$$

Then the elasticity of $x$ with respect to $p$ is

$$\frac{\partial \xi}{\partial \kappa} = \lim_{\Delta\kappa \to 0} \frac{\Delta\xi}{\Delta\kappa} = \left(\frac{p}{x}\right) \lim_{\Delta p \to 0} \frac{\Delta x}{\Delta p} = \left(\frac{p}{x}\right) \frac{\partial x}{\partial p}.$$

We define the elasticity of the $i$th variable with respect to the $k$th parameter, $E_{i,k}$ as

$$E_{i,k} = \frac{p_k(t)}{x_i(t)} \frac{\partial x_i}{\partial p_k}(t). \qquad (51)$$

### *Modeling software*

The model was constructed primarily in R (R Development Core Team 2010) and all figures were produced using its default PDF graphics device. Sensitivity analyses were carried out in MATLAB (MathWorks, Natick, Massachusetts, USA) via the front end software SENSAI (Tavener et al., *in press*), which combines the MATLAB platform and Maple (v14.0; Maplesoft, Waterloo, Ontario, Canada) to calculate derivatives.

## RESULTS

### *Disease-free solutions and sensitivity analysis*

Following a period of transience during regeneration, a disease-free population starting with 1000 $SD_1$ individuals reaches an equilibrium stable stage distribution after approximately 600 years (Fig. 3). The equilibrium stage distribution without disease is $\vec{x}^{\top}_{\{12\}} =$ (62 580, 38, 79, 65, 91, 353, 0, 0, 0, 0, 0, 0), with the total tree population $\sum_{i=2}^{6} x_i = 626$. This equilibrium solution is used in analyses that include rust infection, where we perturb the population from this disease-free equilibrium (see *Introducing WPBR*).

The mature adult stage ($x_6$) quickly dominates the landscape as a result of low mortality and shading effects on younger tree stages and germination rate. The effect of shading through LAI is particularly apparent during the transient phase of regeneration when MA trees decline after ~200 years. The remaining stages respond and increase in size between 300–400 years as a result of increased seed germination (Fig. 3). This equilibrium pine stand closely matches field observations of age structure in high-elevation white pines (Burns 2006; Burns et al. 2011).

Sensitivity analyses with respect to model parameters focused on two quantities: the total population (excluding seeds) and the mature adult population. Analysis of the disease-free population (i.e., regenerating scenario; $\beta = 0$) in Fig. 3 reveals that three sets of parameters have large effects (Fig. 4, top left). Mortality ($p_1, \ldots, p_5$), infection ($p_{10}, \ldots, p_{14}$), and the LAI parameters ($p_{22}$, $p_{23}$) all reduce the MA population, especially in the

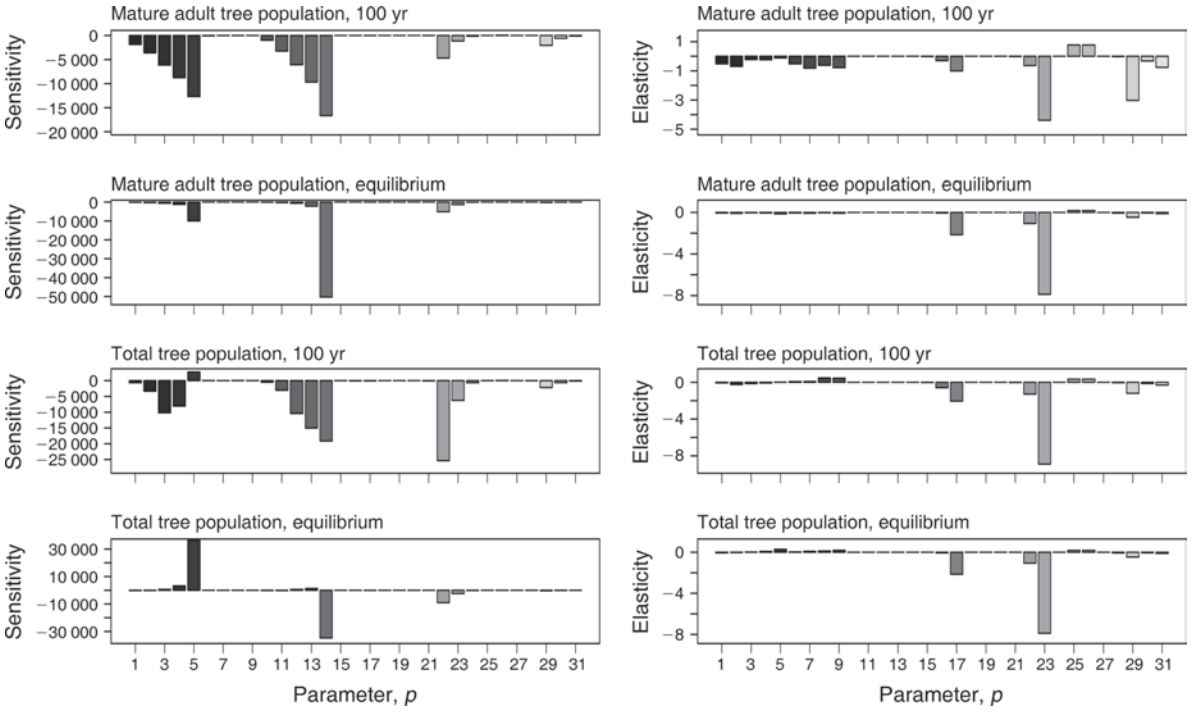


FIG. 4. Sensitivity (left column) and elasticity (right column) plots for the regenerating, disease-free population (Fig. 3). Parameter numbers on the $x$-axis are defined in Table 2. Quantities of interest are both the number of mature adult trees ($x_6$) and the total number of trees ($\sum_{i=2}^{6} x_i$) with respect to each model parameter, at two time steps: during the transient phase of regeneration at 100 years and at the stable equilibrium >1000 years. Bar shading from black to light gray groups associated parameters into clusters to facilitate the identification of related parameters.

transient phase during regeneration when there are relatively few MA individuals. At this time period the MA population depends on younger stages to transition into the MA stage (Fig. 4). At equilibrium, however, the most sensitive parameters for the MA stage are only MA mortality and MA infection probability. Increasing β would have a strong, negative effect on the susceptible MA population as susceptible MA individuals become infected and eventually die.

The total susceptible population ($x_2, \ldots, x_6$) is also sensitive to these same three groups of parameters, both early in the population projection and at equilibrium. The exception is MA mortality ($m_6$), which has a *positive* effect on the total population (Fig. 4, bottom left) as the suppressing effect of density dependence by MA is released.

Elasticity is a rescaling of sensitivity to obtain the *relative* effect of a parameter on the quantity of interest. Model elasticity for MA (Fig. 4, top right) revealed that seed and cone parameters have a positive effect on the MA population. In addition, increasing $P_{\text{find}}$ ($p_{29}$), the proportion of seeds found and consumed by Clark's Nutcrackers, has a negative influence on the MA population. These effects, however, are only important during the transient phase of a regenerating population (i.e., <200 years). Once again, as with the sensitivity, elasticity revealed a consistent pattern of leaf area parameters ($\alpha_2$, $\alpha_3$) with a strong negative effect on both the MA and total populations.

### *Introducing WPBR*

We repeated the analysis with $\beta_i = 0.044$, $i = 2, \ldots, 6$, introducing rust to the disease-free equilibrium population (Fig. 5) and once again examined the mature adult population ($x_6 + x_{12}$) and the total population ($\sum_{i=2}^{12} x_i$) with respect to all model parameters. During the transient phase following infection, elasticities of the parameters revealed a similar pattern to elasticities calculated without infection. Leaf area parameters $\alpha_2$ ($p_{22}$) and $\alpha_3$ ($p_{23}$), seed parameters $C_{\max}$ ($p_{25}$) and $S_{\text{cone}}$ ($p_{26}$), and germination parameters $P_{\text{find}}$ ($p_{29}$) and SpC ($p_{31}$) again had the largest influence. However, the cost of infection to survivorship (δ) becomes a critical parameter. Decreasing infection cost (i.e., increasing δ [$p_{20}$], see Fig. 2d), positively affects the MA population whereas it negatively affects the overall population (Fig. 5a–b).

Lastly, the total tree population becomes sensitive to changes in the mean dbh of mature adults ($p_{17}$). This parameter influences leaf area and thus highlights both the suppressive effects of density-dependence and the codependence of model parameters. Interestingly, the MA population also becomes sensitive to changes in dbh of adult classes at equilibrium (not shown), because the MA population ultimately depends on a supply of

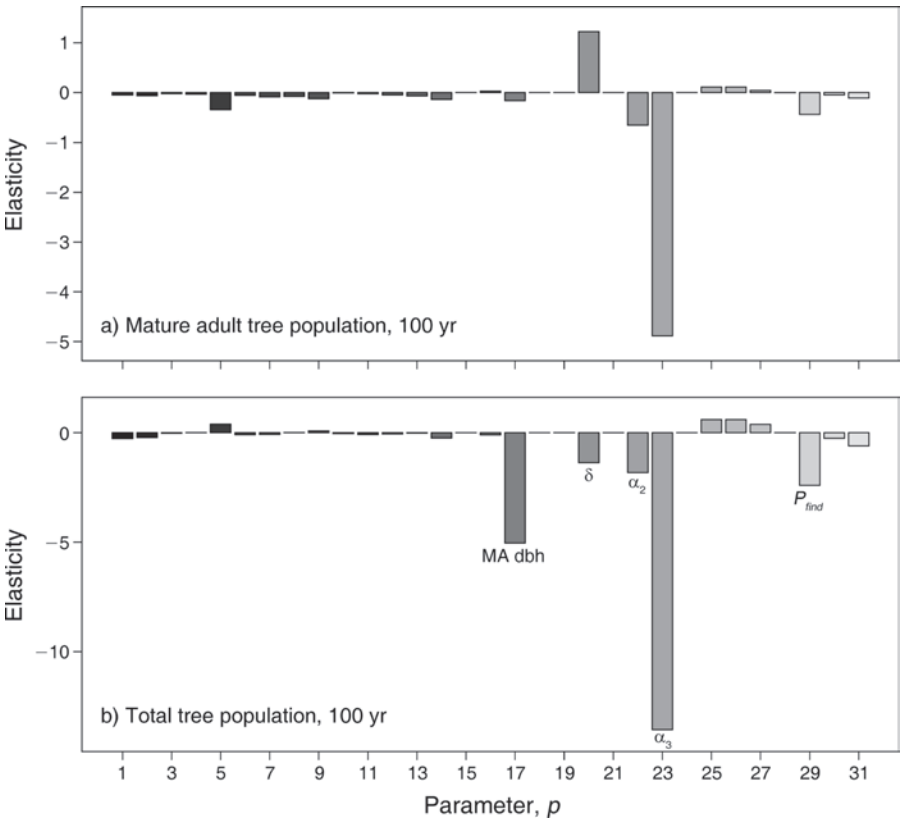


FIG. 5. Elasticity analysis with disease ($\beta_i = 0.044$) during the transience (at 100 years) following infection of a fully susceptible, disease-free equilibrium population (Fig. 3). Quantities of interest are (a) the total mature adult population ($x_6 + x_{12}$) and (b) the total population ($\sum_{i=2}^{12} x_i$). Parameter numbers on the $x$-axis are defined in Table 2. Sensitivities were qualitatively similar (not shown). Note the different scales of the $y$-axes.

seedlings transitioning through the initial stages to become adults. A similar line of reasoning explains the change in magnitude of the seed germination parameters $P_{\text{find}}$ ($p_{29}$), $P_{cons}$ ($p_{30}$), and SpC ($p_{31}$). Mature adults depend indirectly on these parameters as seedlings eventually transition to become adults, whereas the total population includes many early stages that depend directly on germination.

*Infection probability* (β).—As predicted by the sensitivity analysis, introducing disease to the equilibrium population dramatically changes the trajectory (Fig. 6) and stage-structure (Fig. 7) of the population. Low values of β actually have a *positive* effect on the total population as infected MA individuals suffer increased, infection-induced mortality, allowing other classes to increase in number which again highlights the effect of density-dependence mediated by LAI (Fig. 6a). With low β, there are more trees overall, but the population has a vastly different stage structure. This can be seen in Fig. 6b where β has a consistent, negative effect on the MA population. Higher values of β (>0.10) have a consistent, negative effect on the entire population and results in eventual extinction.

Fig. 7 depicts the effect of β on the population trajectory and structure during the transient phase following infection for low ($\beta = 0.016$), medium (the MLE; $\beta = 0.044$), and high ($\beta = 0.20$) transmission probabilities. Following rust introduction a rapid deviation from the initial equilibrium stage structure occurs as the population shifts towards younger stages. At lower β (<0.10), the density-dependent effects of LAI predominate, and increased mortality in adults allows younger stages to increase. However, when $\beta = 0.20$, the population declines deterministically to extinction because infection overcomes the positive effects of removing density-dependent mechanisms on smaller tree stages.

This effect is even greater with additional interspecific competition via $LAI_b$ (Fig. 7e–h). This background shading prevents the population from reaching a viable stable equilibrium even at low transmission probabilities (Fig. 7b–c vs. f–g) as competition from other tree species inhibits seed germination and the supply of younger individuals to the higher stages.

*Infection cost* (δ).—The strength of the infection cost is mediated by the coefficient δ (Fig. 2d). As predicted by the elasticity analysis (Fig. 5), lowering the cost of infection (δ ↑) has a positive effect on the MA population. Conversely, increasing the cost of infection (δ ↓) has a positive effect on the total population

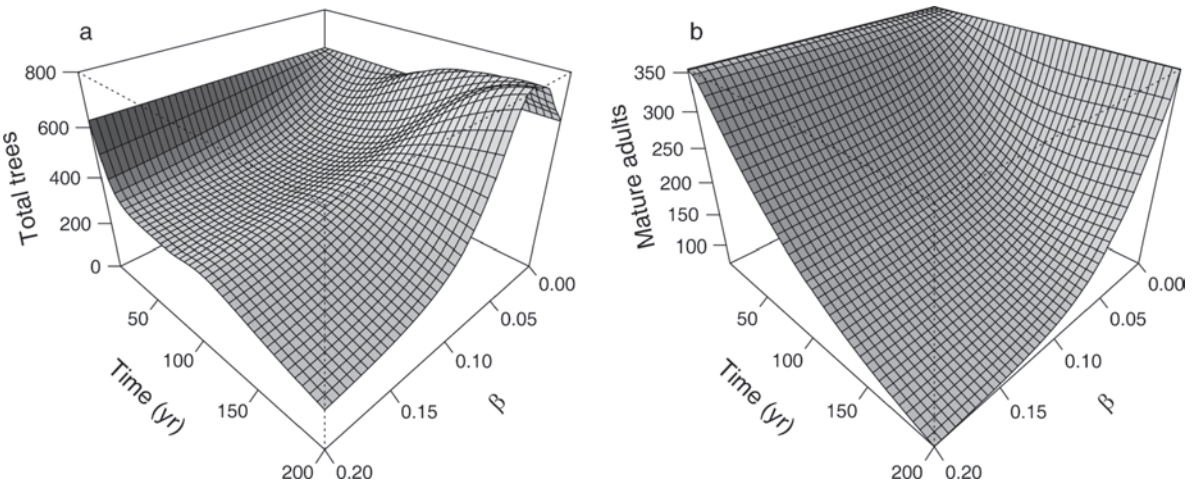


FIG. 6. (a) Surface plot of the total population ($\sum_{i=2}^{12} x_i$) as a function of infection probability (β) and time and (b) surface plot of the total mature adults MA ($x_6 + x_{12}$) as a function of β and time. Initial conditions were the disease-free equilibrium solution (Fig. 3).

(compare Fig. 8a vs. 8b). This is reflected by the change in sign of the elasticities of δ ($p_{20}$) in Fig. 5a and 5b. Simultaneously considering both δ and β further supports this relationship (Fig. 9). With low β and low δ (high cost), the total population increases dramatically in the first 100 years. However when both the infection probability and the cost of infection are high (front corner of Fig. 9), the total population rapidly goes extinct. The suppressive density-dependent effect of mature adults on the rest of the population is eventually overwhelmed by WPBR infection. A similar pattern is observed at equilibrium for both the total and mature adult populations, but extinction occurs in a much larger region of parameter space. This indicates that 100 years is too early in the trajectory to encapsulate population extinction (compare right corner of Fig. 9b and 9d).

*Rust prevalence* (Φ).—We define the stage-specific and total prevalence as the proportion infected individuals defined by

$$\Phi_i = \frac{x_{6+i}}{x_i + x_{6+i}} \qquad i = 2, \ldots, 6 \tag{52}$$

and

$$\Phi_T = \frac{\sum_{i=8}^{12} x_i}{\sum_{i=2}^{12} x_i} \tag{53}$$

respectively. When introduced into a fully susceptible equilibrium population, the total prevalence ($\Phi_T$) rapidly increased for all three values of β (Fig. 10). High infection prevalence is maintained in the MA stage ($\Phi_6$) because they have lower cost of infection and are longer lived than other tree stages and more opportunities to become infected. For $\beta = 0.20$, MA infection prevalence quickly reaches 100% as all trees become infected in the years leading up to adulthood (90 years; Fig. 10c). Because all stages are infected with the same probability (Eq. 44), smaller tree stages also become infected, but suffer such a high cost that they are quickly removed from the population. Fig. 11 shows the cumulative sum of dead seedling ($SD_1$) individuals during the transient phase following rust introduction into an equilibrium population. For high β, the majority of $SD_1$ individuals either die or transition to the $SD_2$ stage. Thus the combined effect of infection-induced mortality and short residence time maintains a low-infected $SD_1$ ($x_8$) population (i.e., low $\Phi_2$).

## DISCUSSION

We analyzed sensitivity and elasticity of a stage-structured, nonlinear disease model of a high-elevation white pine stand in the face of infection with WPBR. In the absence of genetic resistance, our model shows that sustainability of high-elevation white pine stands infected with WPBR depends on two dominant effects: infection probability and regeneration-mediated via competition (e.g., LAI). Parameters controlling these effects disproportionately remove smaller stages via infection induced mortality and by limiting seedling establishment. More generally, parameters and factors that reduce the seedling population impede long-term population viability. Sensitivity analysis further highlights the codependence of model parameters, as some parameters indirectly influence the seedling population through other parameters and/or factors, particularly those involved in density dependence. For example, mean dbh of mature adults ($p_{17}$), suppresses population growth because it is the largest contributor to the leaf area calculation Eq. 23, and contributes to LAI and ultimately the suppression of the regeneration cycle. The potential for parameter codependence in complex,

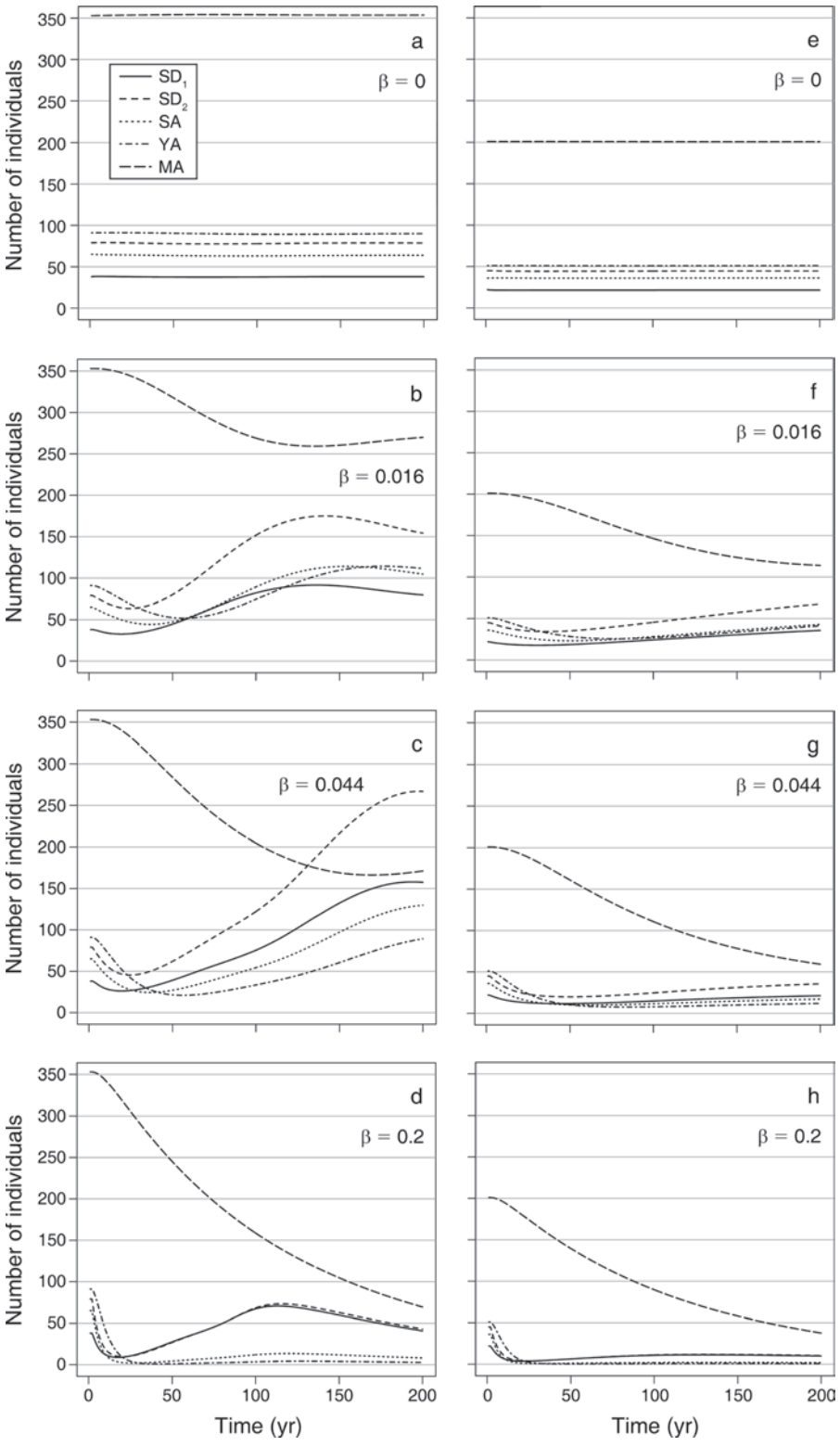


FIG. 7. Population projections and stand structure (a–d) without additional shading from other tree species, background leaf area index $LAI_b = 0$, and (e–h) with shading by other trees, $LAI_b = 2$. Initial conditions were the disease-free equilibrium (Fig. 3). From top to bottom $\beta = 0$, 0.016, 0.044, and 0.20, corresponding to zero, low, medium, and high infection probability. All other parameters were set to default values.

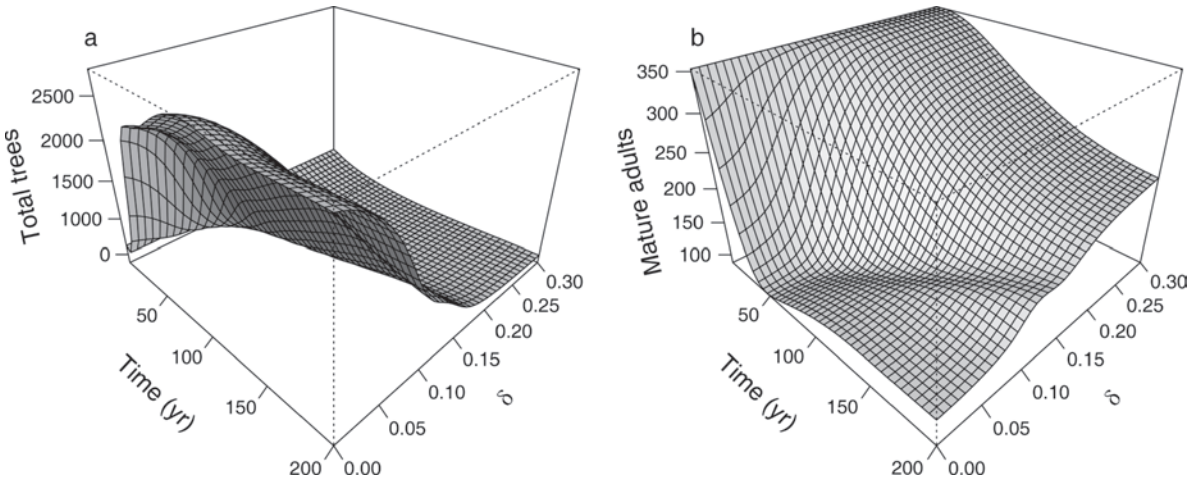


FIG. 8. (a) Surface plot of the total population ($\sum_{i=2}^{12} x_i$) as a function of both the cost of infection (δ) and time and (b) surface plot of the total mature adults ($x_6 + x_{12}$) as a function of δ and time. The default $\delta = 0.15$. A low value of delta corresponds to a high cost of infection (Fig. 2d). Initial conditions were the disease-free equilibrium (Fig. 3); all other parameters set to default values.

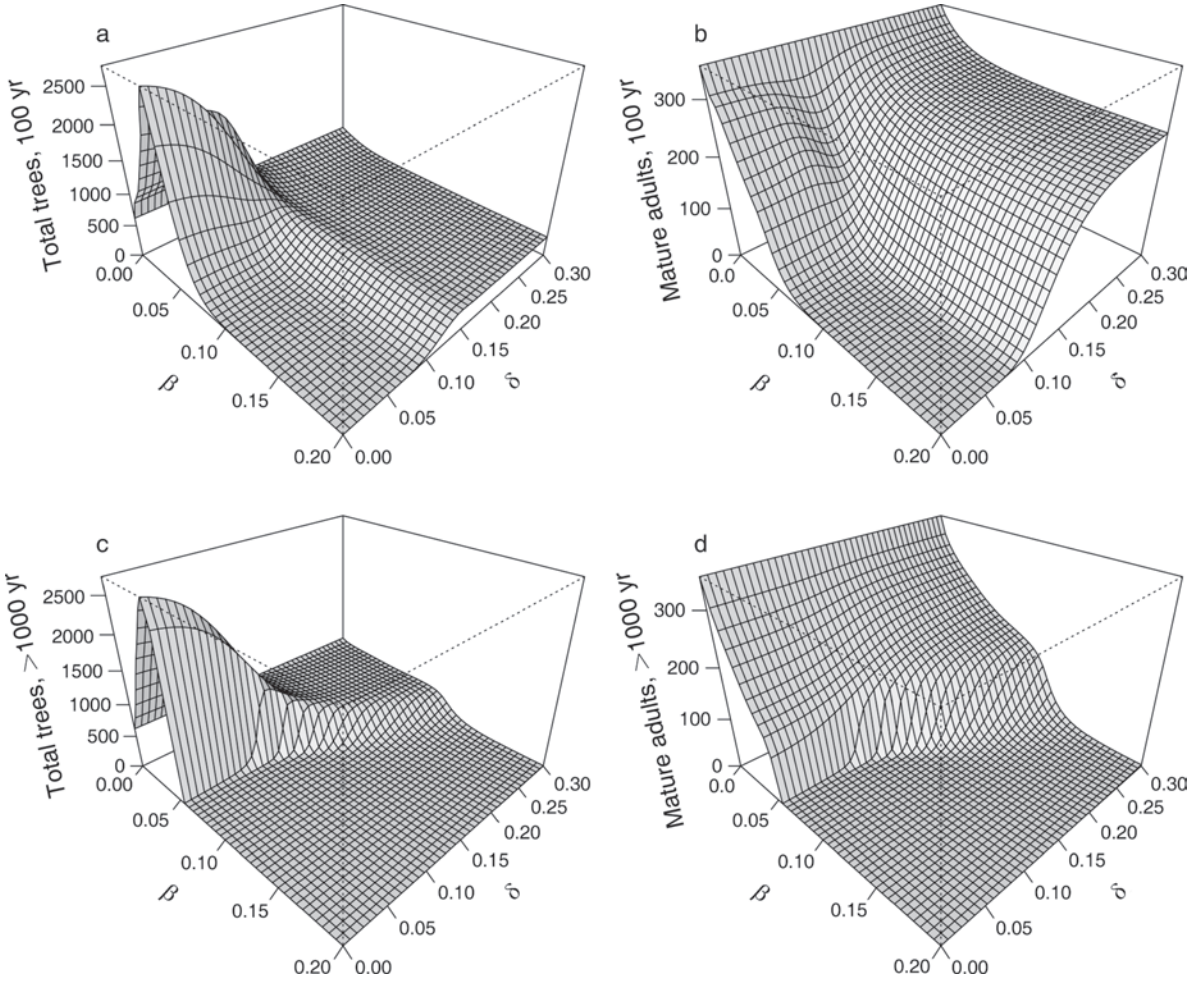


FIG. 9. Surface plots of the relationship between probability of infection (β), the cost of infection coefficient (δ), and the total population ($\sum_{i=2}^{12} x_i$) and mature adults ($x_6 + x_{12}$): (a, b) 100 years after infection was introduced, and (c, d) >1000 years after infection was introduced. The front corner of the graphs represents high probability of infection and high cost of infection, while the back is low probability of infection and low cost of infection.

nonlinear models highlights an advantage of the sensitivity analysis performed here, that unexpectedly influential parameters can be readily identified.

We considered two time steps at which to perform sensitivity analyses: during transience at 100 years and at equilibrium (>1000 years), because sensitivities at these time steps tell us different things about the dynamics of the system. Early transient dynamics are important for analysis of a stand in a state of flux following disturbance (e.g., fire or rust introduction), whereas sensitivities at equilibrium relate to processes in stable, subalpine stands. Further, transient dynamics are likely more informative for management strategies on a realistic timescale. For example, at 100 years, MA individuals are sensitive to both the mortalities and infection probabilities of *all* stages beneath them because adult stages in a regenerating population arise from the supply of smaller stages transitioning into the MA stage (Fig. 4, left). At equilibrium, however, the MA stage is only sensitive to changes in the mortality and infection probability of its *own* stage (i.e., $p_5$ and $p_{14}$). This pattern is even more apparent when one considers the total susceptible population (bottom two of Fig. 4, left). Initially the population is sensitive to numerous parameters related to mortality and infection, but at equilibrium the population as a whole is most sensitive to the mortality and infection of MA only, the stage that dominates at equilibrium.

Starting with the disease-free equilibrium and default parameters, an infected high-elevation white pine population reaches a new diseased equilibrium in less than 500 years, however with a stage distribution that is much less dominated by mature adults. Increasing infection probability (up to $\beta \approx 0.07$) causes a shift in age structure towards younger age classes. Fig. 7 suggests that high-elevation white pine populations are indeed capable of tolerating moderate levels of WPBR infection as long as seedling recruitment is maintained and stands are not simultaneously suppressed by other competing tree species or other agents of mortality (e.g., mountain pine beetle, *Dendroctonus ponderosae*).

Traditional stability analysis of SIR models includes the index $R_0$, the basic reproductive ratio, which is a measure of the linear stability (or instability) of the disease-free equilibrium solution (Keeling and Rohani 2008). In contrast to density- and frequency-dependent disease models that include terms like $SI/N$ or $SI$, our model assumes that infection is from an evenly distributed cloud of spores from alternate hosts (i.e., *Ribes* spp.). The life cycle of WPBR does not involve direct tree-to-tree transmission, so the assumption of a constant $\beta$, independent of the population, seems reasonable. However, a non-trivial disease-free equilibrium solution only exists for the special case when $\beta = 0$ (i.e., the absence of *Ribes*). In this case, the equilibrium solution is always stable with respect to perturbation with infected individuals ($R_0 < 1$), since there is no transmission pathway when $\beta = 0$. In this context, the

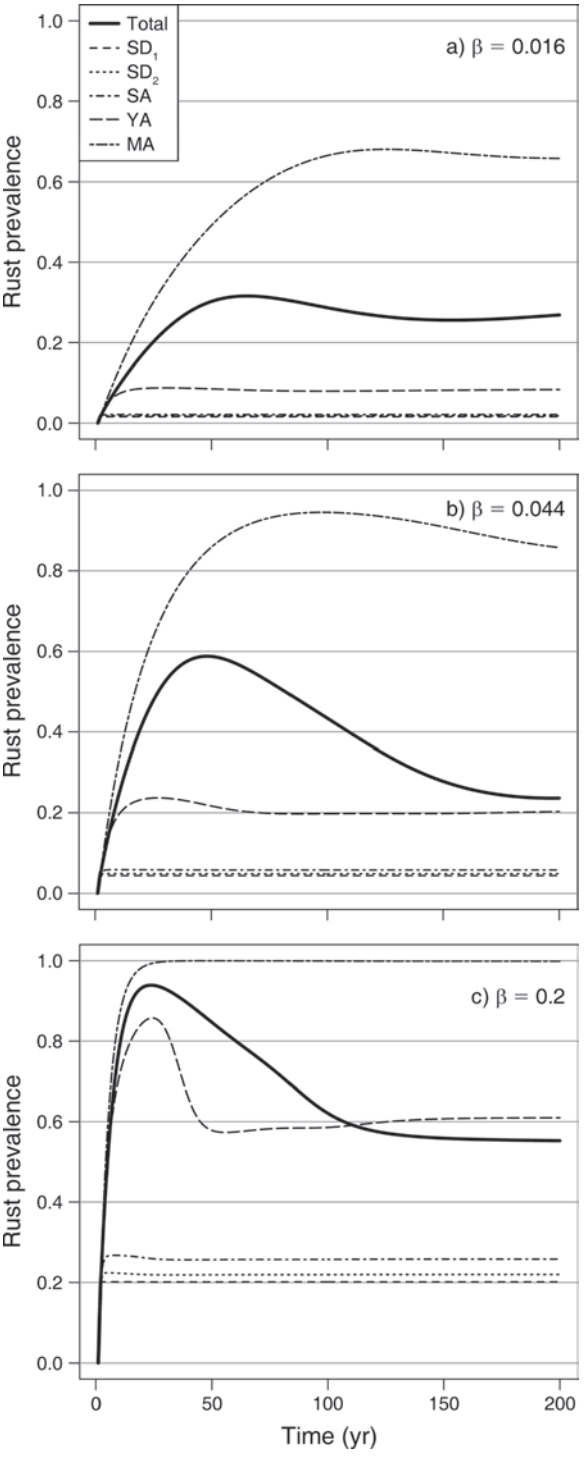


FIG. 10. Stage-specific prevalence ($\Phi_i$, $i = 2, \ldots, 6$) and total prevalence ($\Phi_T$) of white pine blister rust (WPBR) for low ($\beta = 0.016$), medium (the maximum-likelihood estimate [MLE]; $\beta = 0.044$), and high ($\beta = 0.20$) probability of infection over time. The bold solid line represents the overall (total) prevalence of WPBR in the population.

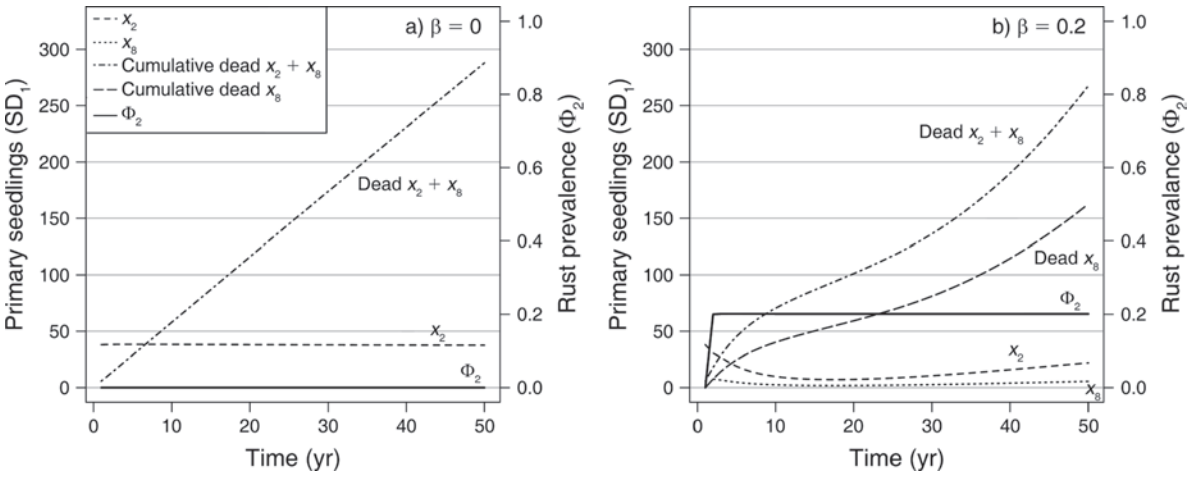


FIG. 11. Population projections for the $SD_1$ class only ($x_2$ and $x_8$) introducing WPBR to an equilibrium structured population. The cumulative sum of dead individuals and the WPBR prevalence of $SD_1$ ($\Phi_2$) is also shown for (a) $\beta = 0$ and (b) high infection probability, $\beta = 0.20$.

traditional notion of $R_0$ is defined, but uninformative because any infected individuals introduced to the population simply die out. In our model, the appropriate analogue is not equilibrium stability with respect to adding infected individuals, but rather stability with respect to the addition of infected *Ribes* which complete the transmission pathway. For this class of model, an alternative measure of the population's susceptibility to disease could be the sensitivity of the diseased population ($\sum_{i=8}^{12} x_i$) with respect to transmission probability ($\beta$) when $\beta = 0$.

Rust prevalence in the $SD_1$ ($\Phi_2$) is low when infection probability $\beta = 0.044$, yet primary seedlings become infected (4.4%/year). Rust prevalence remains low because of the combination of high infection cost, high natural mortality, and low residence time (Fig. 11). Therefore, in natural populations, the $SD_1$ population may appear uninfected (or escaping infection), but our model suggests infected $SD_1$ simply do not remain long enough, either as dead trees on the landscape or as transitioned maturing seedlings, to be reliably sampled. This may account for the low seedling rust prevalence found in field surveys (Kearns 2005, Burns 2006). The converse is also true. The model predicts that the stage with the largest residence time and the lowest mortality will accumulate the highest rust prevalence in the population, namely the mature adults (Fig. 10). High rust prevalence in larger size classes has been observed by Conklin (2004) in *P. strobiformis*, Burns et al. (2011) in *P. flexilis*, and Smith and Hoffman (2000) in *P. albicaulis*.

This model lays the framework for studying WPBR infection in a stage-structured, deterministic, nonlinear map, but could be extended to include broader ecosystem interactions or disturbances via external forces (e.g., the effect of climate on seedling establishment). Further, alternative infection dynamics could be incorporated (e.g., density-dependent infection) as well as age of infection, multiple infections, and location of infections on trees. Finally, heritable resistance to WPBR has been described at low frequency in high-elevation white pines (Hoff et al. 1980), and may include a mechanism that is controlled by a single dominant gene (Kinloch and Dupper 2002). Using the mathematical framework developed in Tavener et al. (*in press*) this model can be readily extended to include single-locus genetics as an additional nonlinearity. The effect of genetic resistance in this host-pathogen system is the basis of forthcoming papers.

## CONCLUSIONS

Our model clearly demonstrates a strong effect of WPBR on population structure. The sensitivity and elasticity analyses indicate that future research should focus on improving estimates of both infection probability and infection cost. They also suggests the exploration of the effects of competition (i.e., density dependence) on population dynamics, especially seedling recruitment, is warranted. These efforts should be used to develop management strategies to mitigate these effects. For example, stimulating natural regeneration or planting genetically resistant individuals, which have been suggested as potentially critical management solutions (Schoettle and Sniezko 2007), would likely lower the effects of both infection probability and cost, especially if infection is found to be density dependent as suggested by Hatala et al. 2011.

We further propose an alternative interpretation to field observations of both high prevalence in larger sized trees and particularly low prevalence in young (e.g., $SD_1$) size classes. Prevalence in younger stages may be low not because of a low infection probability, as previously assumed, but caused by a combination of high infection cost and short residence time (and vice

versa for larger trees). If so, a more careful evaluation of seedling mortality could reveal additional management strategies.

Our model provides an example of how sensitivity analysis can be used to determine critical parameters in complex, nonlinear models under transient and/or equilibrium conditions in an applied ecological context.

Acknowledgments

We thank the following for primary or unpublished data: K. Burns, D. Conkin, J. Coop, M. Germino, A. Sala, and D. Tomback. We thank B. Keane, S. McKinney, and R. Sniezko for insightful discussions. Funding was provided by USDA Forest Service Rocky Mountain Research Station (#07-RJVA-11221616-252) to M. F. Antolin and USDA Economic Research Service Program of Research on the Economics of Invasive Species Management (PREISM: #58-7000-8-0096) to A. W. Schoettle. We thank members of the "Flexible and Extendible Scientific Undergraduate Experience" program (FESCUE) for valuable discussions and model development. Last, the final version of the manuscript was greatly improved by comments from two anonymous reviewers.

Literature Cited

Anderson, R. M., and R. M. May. 1979. Population biology of infectious diseases. Nature 280:361–367.

Anderson, R. M., and R. M. May. 1986. The invasion persistence and spread of infectious diseases within animal and plant communities. Philosophical Transactions of the Royal Society B 314:533–570.

Brown, D. 2001. A spectral unmixing approach to leaf area index (LAI) estimation at the alpine treeline ecotone. Pages 7–21 *in* A. Millington, S. Walsh, and P. Osborne, editors. GIS and remote sensing applications in biogeography and ecology. Kluwer, Dordrecht, The Netherlands.

Burns, K. S. 2006. White pine blister rust surveys in the Sangre de Cristo and wet mountains of southern Colorado. Technical Report R2-06-05. USDA Forest Service, Denver, Colorado, USA.

Burns, K. S., J. Blodgett, M. Jackson, B. Howell, W. R. Jacobi, A. W. Schoettle, A. M. Casper, and J. G. Klutsch. 2011. Monitoring limber pine health in the Rocky Mountains and North Dakota. Pages 47–50 *in* R. E. Keane, D. F. Tomback, M. P. Murray, and C. M. Smith, editors. The future of high-elevation, five-needle white pines in Western North America: Proceedings of the High Five Symposium, 28–30 June 2010, Missoula, Montana. Proceedings RMRS-P-63. USDA Forest Service, Rocky Mountain Research Station, Fort Collins, Colorado, USA.

Callaway, R., A. Sala, and R. Keane. 2000. Succession may maintain high leaf area: sapwood ratios and productivity in old subalpine forest. Ecosystems 3:254–268.

Caswell, H. 2001. Matrix population models: construction, analysis, and interpretation. Second edition. Sinauer Associates, Sunderland, Massachusetts, USA.

Caswell, H. 2007. Sensitivity analysis of transient population dynamics. Ecology Letters 10:1–15.

Caswell, H. 2008. Perturbation analysis of nonlinear matrix population models. Demographic Research 18:59–116.

Conklin, D. 2004. Development of the white pine blister rust outbreak in New Mexico. Technical Report R3-04-01. USDA Forest Service, Albuquerque, New Mexico, USA.

Cottone, N. 2001. Modeling whitebark pine infected with blister rust in Mt. Rainier National Park, WA. Thesis. St. Joseph's University, Philadelphia, Pennsylvania, USA.

Crowl, T. A., T. O. Crist, R. R. Parmenter, G. Belovsky, and A. E. Lugo. 2008. The spread of invasive species and infectious disease as drivers of ecosystem change. Frontiers in Ecology and the Environment 6:238–256.

Ettl, G., and N. Cottone. 2004. Whitebark pine (*Pinus albicaulis*) in Mt. Rainier National Park: response to blister rust infection. Pages 36–47 *in* H. Akçakaya, M. Burgman, O. Kindvall, C. Wood, P. Sjögren-Gulve, J. Hatfield, and M. McCarthy, editors. Species conservation and management. Oxford University Press, New York, New York, USA.

Ezard, T. H. G., J. M. Bullock, H. J. Dalgleish, A. Millón, F. Pelletier, A. Ozgul, and D. N. Koons. 2010. Matrix models for a changeable world: the importance of transient dynamics in population management. Journal of Applied Ecology 47:515–523.

Fox, G. A., and J. Gurevitch. 2000. Population numbers count: tools for near-term demographic analysis. American Naturalist 156:242–256.

Gower, S. T., C. J. Kucharik, and J. M. Norman. 1999. Direct and indirect estimation of leaf area index, fapar, and net primary production of terrestrial ecosystems. Remote Sensing of Environment 70:29–51.

Haridas, C., and S. Tuljapurkar. 2007. Time, transients and elasticity. Ecology Letters 10:1143–1153.

Hatala, J., M. Dietze, R. Crabtree, K. Kendall, D. Six, and P. Moorcroft. 2011. An ecosystem-scale model for the spread of a host-specific forest pathogen in the greater Yellowstone ecosystem. Ecological Applications 21:1138–1153.

Hoff, R., R. Bingham, and G. McDonald. 1980. Relative blister rust resistance of white pines. European Journal of Forest Pathology 10:307–316.

Hoff, R., and S. Hagle. 1990. Disease of whitebark pine with special emphasis on white pine blister rust. Pages 179–190 *in* W. Schmidt and K. MacDonald, editors. Proceedings of the symposium on whitebark pine ecosystems: ecology and management of a high mountain resource. General Technical Report INT-270. U.S. Department of Agriculture Forest Service, Ogden, Utah, USA.

Keane, R., S. Arno, J. Brown, and D. Tomback. 1990. Modelling stand dynamics in whitebark pine (*Pinus albicaulis*) forests. Ecological Modelling 51:73–95.

Keane, R., P. Morgan, and S. Running. 1996. Fire-BGC: a mechanistic ecological process model for simulating fire succession on coniferous forest landscapes of the northern Rocky Mountains. Research Paper INT-RP-484. U.S. Department of Agriculture, Forest Service, Intermountain Research Station, Ogden, Utah, USA.

Kearns, H. S. J. 2005. White pine blister rust in the central Rocky Mountains: modeling current status and potential impacts. Dissertation. Colorado State University, Fort Collins, Colorado, USA.

Keeling, M., and P. Rohani. 2008. Modeling infectious diseases in humans and animals. Princeton University Press, Princeton, New Jersey, USA.

Keeling, M., M. Woolhousae, R. May, G. Davies, and B. Grenfell. 2003. Modelling vaccination strategies against foot-and-mouth disease. Nature 421:136–142.

Kegley, A., and R. Sniezko. 2004. Variation in blister rust resistance among 226 *Pinus monticola* and s217 *P. lambertiana* seedling families in the Pacific Northwest. Pages 209–226 *in* R. Sniezko, S. Samman, S. Schlarbaum, and H. Kriebel, editors. Breeding and genetic resources of five-needle pines: growth adaptability and pest resistance. Proceedings RMRS-P-32, Fort Collins, CO edition. IUFRO Working Party 2.02.15, USDA Forest Service, Rocky Mountain Research Station, Medford, Oregon, USA.

Kinloch, B., and G. Dupper. 2002. Genetic specificity in the white pine-blister rust pathosystem. Phytopathology 92:278–280.

Law, B., S. van Tuyl, A. Cescatti, and D. Baldocchi. 2001. Estimation of leaf area index in open-canopy ponderosa pine forests at different successional stages and management regimes in Oregon. Agricultural and Forest Meteorology 108:1–14.

Maher, E., and M. Germino. 2006. Microsite differentiation among conifer species during seedling establishment at alpine treeline. Ecoscience 13:334–341.

McCaughey, W., and W. Schmidt. 1990. Autecology of whitebark pine. Pages 85–96 *in* W. Schmidt and K. McDonald, editors. Proceedings, symposium on whitebark pine ecosystems: ecology and management of a high-mountain resource. General Technical Report INT-270. USDA Forest Service Intermountain Research Station, Ogden, Utah, USA.

McKinney, S., and D. Tomback. 2007. The influence of white pine blister rust on seed dispersal in whitebark pine. Canadian Journal of Forest Research 37:1044–1057.

Oli, M., M. Venkataraman, P. Klein, L. Wendland, and M. Brown. 2006. Population dynamics of infectious diseases: a discrete time model. Ecological Modelling 198:183–194.

Pease, C., and D. Mattson. 1999. Demography of the Yellowstone grizzly bears. Ecology 80:957–975.

R Development Core Team. 2010. R: a language and environment for statistical computing (v2.11.1). R Foundation for Statistical Computing, Vienna, Austria. http://www.R-project.org

Schoettle, A. W. 1994. Influence of tree size on shoot structure and physiology of *Pinus contorta* and *Pinus aristata*. Tree Physiology 14:1055–1068.

Schoettle, A. W. 2004. Ecological roles of five-needle pines in Colorado: potential consequences of their loss. Pages 124–135 *in* R. Sniezko, S. Samman, S. Schlarbaum, and B. Howard, editors. Breeding and genetic resources of five-needle pines: growth, adaptability and pest resistance. RMRS-P-32. USDA Forest Service Proceedings, Rocky Mountain Forest and Range Experimental Station, Fort Collins, Colorado, USA.

Schoettle, A., and S. Rochelle. 2000. Morphological variation of *Pinus flexilis* (Pinaceae), a bird-dispersed pine, across a range of elevations. American Journal of Botany 87:1797–1806.

Schoettle, A. W., and R. A. Sniezko. 2007. Proactive intervention to sustain high-elevation pine ecosystems threatened by white pine blister rust. Journal of Forest Research 12:327–336.

Schwartz, C., M. Haroldson, G. White, R. Harris, S. Cherry, K. Keating, D. Moody, and C. Servheen. 2006. Temporal, spatial, and environmental influences on the demographics of grizzly bears in the greater Yellowstone ecosystem. Wildlife Monographs 161:1–68.

Shepperd, W., C. Edminster, and S. Matta. 2006. Long-term seedfall, establishment, survival, and growth of natural and planted Ponderosa pine in the Colorado front-range. Western Journal of Applied Forestry 21:19–26.

Smith, C., B. Wilson, S. Rasheed, R. Walker, T. Carolin, and B. Shepherd. 2008. Whitebark pine and white pine blister rust in the Rocky Mountains of Canada and northern Montana. Canadian Journal of Forest Research 38:982–995.

Smith, J., and J. Hoffman. 2000. Status of white pine blister rust in the intermountain west. Western North American Naturalist 60:165–179.

Smith, J., and J. Hoffman. 2001. Site and stand characteristics related to white pine blister rust in high-elevation forests of southern Idaho and western Wyoming. Western North American Naturalist 64:409–416.

Steltzer, H., and J. Welker. 2006. Modeling the effects of photosynthetic vegetation properties on the NDVI–LAI relationship. Ecology 87:2765–2772.

Tavener, S. J., M. Mickucki, S. G. Field, and M. F. Antolin. *In press*. Transient sensitivity analysis of nonlinear population models. Methods in Ecology and Evolution.

Tomback, D. 1982. Dispersal of whitebark pine seeds by Clark's nutcracker: a mutualism hypothesis. Journal of Animal Ecology 51:451–467.

Tomback, D., and P. Achuff. 2010. Blister rust and western forest biodiversity: ecology, values and outlook for white pines. Forest Pathology 40:186–225.

Tomback, D., A. W. Schoettle, K. Chevalier, and C. Jones. 2005. Life on the edge for limber pine: seed dispersal within a peripheral population. Ecoscience 12:519–529.

Tomback, D., S. Sund, and L. Hoffman. 1993. Post-fire regeneration of *Pinus albicaulis:* height-age relationships, age structure, and microsite characteristics. Canadian Journal of Forest Research 23:113–119.

vander Wall, S. 1988. Foraging of Clark's Nutcrackers on rapidly changing pine seed resources. Condor 90:624–631.

vander Wall, S., and R. Balda. 1977. Co-adaptations of the Clark's Nutcracker and the piñón pine for efficient seed harvest and dispersal. Ecological Monographs 47:89–111.

Woodward, F. 1987. Climate and plant distribution. Cambridge University Press, Cambridge, UK.

## Supplemental Material

### Appendix A

Parameter estimation (*Ecological Archives* A022-010-A1).

### Appendix B

Model assumptions (*Ecological Archives* A022-010-A2).